

# Crystallization studies on rare-earth co-doped fluorozirconate-based glasses

C. Paßlick<sup>a</sup>, J.A. Johnson<sup>b</sup>, S. Schweizer<sup>c,d,\*</sup>

<sup>a</sup>Centre for Innovation Competence SiLi-nano<sup>®</sup>, Martin Luther University of Halle-Wittenberg, Karl-Freiherr-von-Fritsch-Str. 3, 06120 Halle (Saale), Germany

<sup>b</sup>Department of Biomedical Engineering, University of Tennessee Space Institute, Tullahoma, TN 37388, USA

<sup>c</sup>Department of Electrical Engineering, South Westphalia University of Applied Sciences, Lübecker Ring 2, 59494 Soest, Germany

<sup>d</sup>Fraunhofer Center for Silicon Photovoltaics CSP, Walter-Hülse-Str. 1, 06120 Halle (Saale), Germany

## Abstract

This work focuses on the structural changes of barium chloride ( $\text{BaCl}_2$ ) nanoparticles in fluorochlorozirconate-based glass ceramics when doped with two different luminescent activators, in this case rare-earth (RE) ions, and thermally processed using a differential scanning calorimeter. In a first step, only europium in its divalent and trivalent oxidation states,  $\text{Eu}^{2+}$  and  $\text{Eu}^{3+}$ , is investigated, which shows no significant influence on the crystallization of hexagonal phase  $\text{BaCl}_2$ . However, higher amounts of  $\text{Eu}^{2+}$  increase the activation energy of the phase transition to an orthorhombic crystal structure. In a second step, nucleation and nanocrystal growth are influenced by changing the structural environment of the glasses by co-doping with  $\text{Eu}^{2+}$  and trivalent  $\text{Gd}^{3+}$ ,  $\text{Nd}^{3+}$ ,  $\text{Yb}^{3+}$ , or  $\text{Tb}^{3+}$ , due to the different atomic radii and electro-negativity of the co-dopants.

## Keywords:

crystallization, glass ceramics, rare-earth doping, nanocrystals

## 1. Introduction

Recent studies have shown that fluorochlorozirconate (FCZ)-based glasses and glass ceramics doped with rare-earth (RE) ions such as  $\text{Eu}^{2+}$  are good candidates for image plates in medical diagnostics and up- or down-conversion layers for solar cells providing broad and strong blue luminescence upon ultraviolet or x-ray excitation [1, 2, 3, 4, 5].

The  $\text{BaCl}_2$  is crystallized by thermal treatment of the “as-poured” glass leading to nucleation and growth of nanocrystals in the glass matrix, creating a glass ceramic. These few hundred nanometer-sized crystals, in which a part of the luminescent activator ions are incorporated, provide lower phonon frequencies, making non-radiative relaxation processes less probable; this enables an enhanced luminescence yield. It is therefore essential to be able to precisely control the nanocrystallite nucleation and growth. Previous work has shown that the  $\text{BaCl}_2$  crystallization activation energy is affected by RE doping [6]. More general work on crystallization in zirconium fluoride glasses can be found in [7, 8].

At this moment, several routes are being explored to reduce costs of  $\text{Eu}^{2+}$ -doped glasses and to achieve a higher total luminescence output [9, 10]. It was shown that during glass melting cheaper  $\text{Eu}^{3+}$  is partially reduced to the more expensive  $\text{Eu}^{2+}$ , meaning that multivalent doping of  $\text{Eu}^{2+}$  and  $\text{Eu}^{3+}$  in the starting materials can reduce costs.

In an attempt to enhance light output, the  $\text{Eu}^{2+}$  glasses were additionally doped with a further RE, namely Gd, Nd, Yb, or Tb, to study possible energy transfer between the RE dopants

and potential effects on the optical and structural properties. This work focuses on how the varying amounts of divalent and trivalent Eu and the different RE dopants affect the  $\text{BaCl}_2$  crystallization investigated by differential scanning calorimetry (DSC). For medical and photovoltaic applications it is essential to perform DSC measurements on all glass ceramics to be able to optimize the annealing conditions as well as the respective luminescence yield.

## 2. Materials and methods

The investigated fluorochlorozirconate (FCZ) glasses are based on a modified ZBLAN composition [11], which nominally consists of  $51\text{ZrF}_4\text{-}20\text{BaCl}_2\text{-}20\text{NaF}\text{-}3.5\text{LaF}_3\text{-}3\text{AlF}_3\text{-}0.5\text{InF}_3\text{-}x\text{EuCl}_2\text{-(}2\text{-}x\text{)EuCl}_3$  ( $x = 0, 0.4, 0.8, 1.2, 1.6, 2.0$ ) (values in mol%) for the multivalent Eu series and  $51\text{ZrF}_4\text{-}20\text{BaCl}_2\text{-}20\text{NaF}\text{-}3.5\text{LaF}_3\text{-}3\text{AlF}_3\text{-}0.5\text{InF}_3\text{-}1\text{EuCl}_2\text{-}1\text{RECl}_3$  (RE =  $\text{Gd}^{3+}$ ,  $\text{Nd}^{3+}$ ,  $\text{Tb}^{3+}$ ,  $\text{Yb}^{3+}$ ) for the RE co-doping series (values in mol%).

Glass preparation was done under an argon atmosphere inside a glove box. A two-step melting process was used, where the first step involved mixing and melting of all fluorides at  $800^\circ\text{C}$  for 60 minutes. After being cooled to room temperature chlorides were added to the melt and the whole composition was remelted for 60 minutes at  $745^\circ\text{C}$ . The last step involved pouring into a  $200^\circ\text{C}$  hot brass mold, where it stayed for 60 minutes before being cooled to room temperature at  $50^\circ\text{C}$  per hour.

The DSC measurements were performed with a DSC 204 F1 Phoenix instrument (Netzsch). The sample was cut into small pieces of about 20 to 40 mg and then placed in an aluminum

\*Corresponding author

Email address: [schweizer.stefan@fh-swf.de](mailto:schweizer.stefan@fh-swf.de) (S. Schweizer)

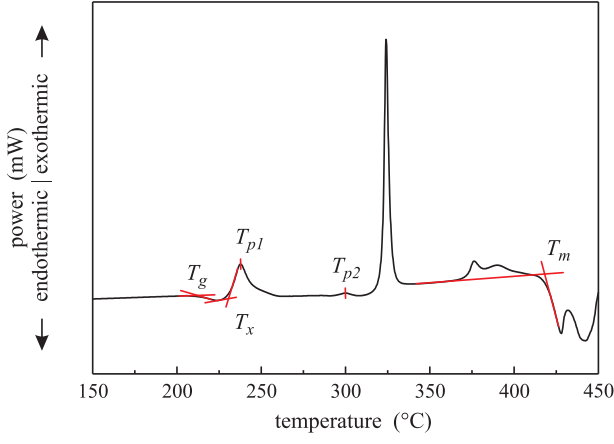


Figure 1: Plot of the DSC data for the FCZ glass with a  $\text{Eu}^{2+}$  fraction of 60%. The heating rate was 10 K/min.

Table 1: Overview of nominal and experimentally determined  $\text{Eu}^{2+}$  fractions for the multivalent Eu-doping series. A nominal  $\text{Eu}^{2+}$  fraction of 100% corresponds to a  $\text{Eu}^{2+}$  doping level of  $x = 2.0$  mol%. The experimental analysis was done by x-ray absorption near edge spectroscopy (XANES) [10]. The respective  $\text{Eu}^{3+}$  fraction is given by  $1 - \text{Eu}^{2+}$ .

nominal $\text{Eu}^{2+}$ fraction (%)	experimental $\text{Eu}^{2+}$ fraction (averaged) (%)
0	$39 \pm 4$
20	$54 \pm 4$
40	$66 \pm 3$
60	$76 \pm 2$
80	$83 \pm 3$
100	$84 \pm 1$

crucible. An empty crucible was used as a reference. The temperature was increased with heating rates of 5, 7.5, 10, 15, 20, and 25 K/min while the differential temperature between the crucibles was measured.

### 3. Results and discussion

#### 3.1. Multivalent Eu-doping

The oxidation state's influence on the crystallization is shown by non-isothermal DSC measurements. The important points of interest are marked in Figure 1 for an FCZ glass with an  $\text{Eu}^{2+}$  fraction of 60%, measured with a heating rate of 10 K/min.  $T_g$  is the glass transition temperature, i.e., the point where glass viscosity and specific heat capacity drop significantly. The crystallization onset,  $T_x$ , and the peak temperature of the first crystallization,  $T_{p1}$ , are attributed to the crystallization of hexagonal  $\text{BaCl}_2$ , while  $T_{p2}$  is attributed to the phase transition from hexagonal to orthorhombic  $\text{BaCl}_2$ .

In previous work, x-ray absorption near-edge structure spectroscopy (XANES) was used to evaluate  $\text{Eu}^{2+}$ -to- $\text{Eu}^{3+}$  ratios, accurately. Nominal and experimentally determined values are summarized in Table 1. The listed experimentally determined

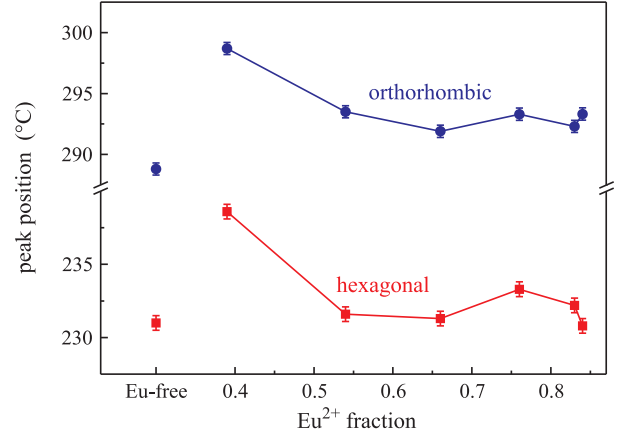


Figure 2: Crystallization peak position for the hexagonal (squares) and the orthorhombic  $\text{BaCl}_2$  crystallization (circles) depending on the different  $\text{Eu}^{2+}$  and  $\text{Eu}^{3+}$  doping fractions. The heating rate was 5 K/min. Data for a Eu-free ZBLAN glass is shown for comparison.

value is the average of all ratios of the as-made and the differently annealed samples having the same composition. A detailed description of the analysis and the experimental details can be found in [10]. Figure 2 shows the peak temperature of both hexagonal and orthorhombic peak maxima as a function of the different  $\text{Eu}^{2+}$ -to- $\text{Eu}^{3+}$  doping fractions; the heating rate was 5 K/min. A significant shift to lower temperatures is observed for both peaks when increasing the  $\text{Eu}^{2+}$  fraction from 0% to 20%. This trend confirms the behavior of the phase transition temperature obtained from corresponding x-ray diffraction (XRD) data of the heat treated samples [10]: For pure  $\text{EuCl}_3$  doping, higher annealing temperatures are required to convert the hexagonal particles into particles with orthorhombic crystal structure. The hexagonal phase results from 20 minute heat treatments between 250 to 270 °C; at 280 °C a phase mixture of hexagonal and orthorhombic phase is found, while the fully crystallized orthorhombic phase is not observed before 290 °C. Crystallization peak positions for a Eu-free ZBLAN glass are shown for comparison. Averaging the peak temperatures of the Eu-doped samples shows that Eu doping leads to a higher temperature shift for the transformation to the orthorhombic phase ( $T_{p2} = 289$  °C for the Eu-free sample to  $\bar{T}_{p2} = 294$  °C for the Eu-doped samples) than for the hexagonal phase crystallization ( $T_{p1} = 231$  °C for the Eu-free sample to  $\bar{T}_{p2} = 233$  °C for the Eu-doped samples). This behavior is described in more detail below.

DSC measurements with different heating rates,  $\alpha$ , enable the determination of the  $\text{BaCl}_2$  crystallization activation energy,  $E_a$ , by Kissinger's method [12]:

$$\frac{d[\ln(\alpha/T_p^2)]}{d(1/T_p)} = -\frac{E_{a,\text{Kissinger}}}{R} \quad (1)$$

where  $R$  is the gas constant. With higher heating rates the crystallizations are shifted to higher temperatures; their peak intensities are increased due to an enhanced heat flow  $dH_c/dT$  into the samples (see Figure 3), which is given by the product

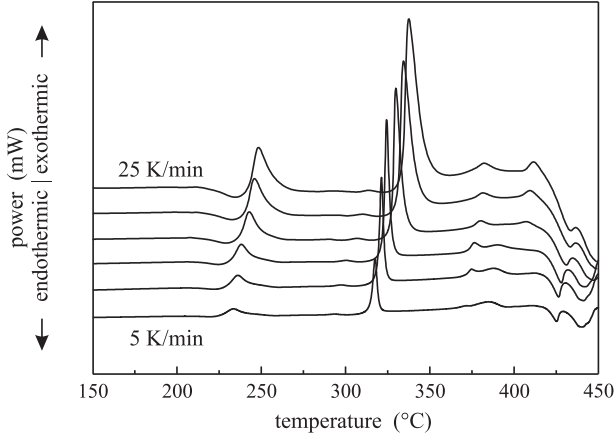


Figure 3: Plot of the DSC data for the FCZ glass with a  $\text{Eu}^{2+}$  fraction of 80%. The different heating rates go from 5, 7.5 and 10 to 25 K/min in steps of 5 K/min. The curves are vertically displaced for clarity.

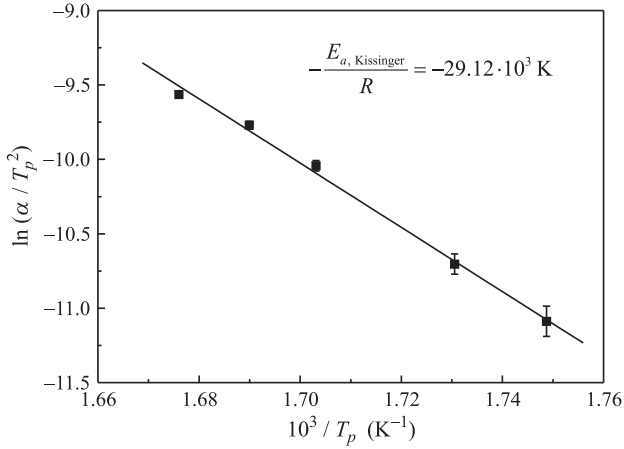


Figure 4: Fit for the pure  $\text{EuCl}_3$ -doped FCZ glass. The slope gives the apparent activation energy,  $E_a$ .

$$dH_c/dT = m \cdot c_p \cdot \alpha \quad (2)$$

with the sample mass,  $m$ , the sample specific heat capacity,  $c_p$ , and the constant heating rate,  $\alpha$ . When plotting  $\ln(\alpha/T_p^2)$  vs.  $(1/T_p)$  as shown in Figure 4,  $E_a$  can be obtained from the slope of the linear fit.

Figure 5 shows  $E_a$  versus  $\text{Eu}^{2+}$  and  $\text{Eu}^{3+}$  doping fraction.  $E_a$  of the hexagonal phase is not sensitive to different Eu oxidation states, but  $E_a$  of the hexagonal to orthorhombic phase transformation shows an increase with increasing  $\text{Eu}^{2+}$  amount, i.e., more energy is needed to initialize the transformation to orthorhombic crystal structure. However, some points trend down, likely caused by composition inhomogeneities from pieces coming from different sample positions.

Compared to the pure  $\text{EuCl}_2$ -doped FCZ glass ( $\text{Cl}/(\text{Cl}+\text{F}) = 15.22\%$ ) the available  $\text{Cl}/(\text{Cl}+\text{F})$  amount in the melt is 0.6% higher for pure  $\text{EuCl}_3$  doping (15.81%), i.e., the small increase in the chlorine volume fraction for changing the Eu-doping from  $\text{Eu}^{2+}$  to  $\text{Eu}^{3+}$  could be the reason for the fact that the en-

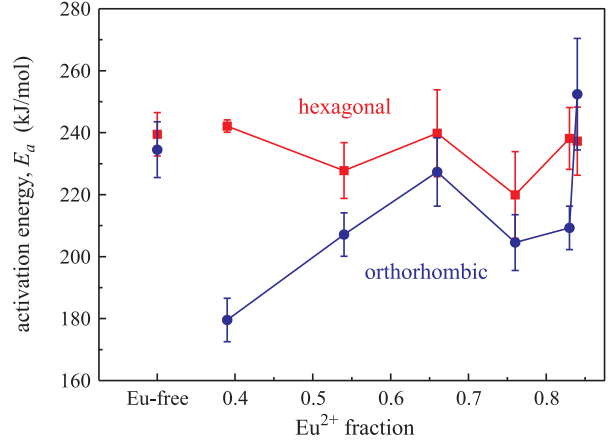


Figure 5: Activation energies,  $E_a$ , for the hexagonal (squares) and the orthorhombic (circles)  $\text{BaCl}_2$  crystallization obtained from the DSC data depending on the different  $\text{Eu}^{2+}$  and  $\text{Eu}^{3+}$  doping fractions. Data for a Eu-free ZBLAN glass is shown for comparison.

ergy needed for the phase transformation decreases. Furthermore, photoluminescence measurements have shown that  $\text{Eu}^{2+}$  is incorporated into the  $\text{BaCl}_2$  nanocrystals, but  $\text{Eu}^{3+}$  is not [13];  $\text{Eu}^{2+}$  substitutes for  $\text{Ba}^{2+}$  in  $\text{BaCl}_2$  [14]. A higher  $\text{Eu}^{2+}$  doping fraction probably results in a higher  $\text{Eu}^{2+}$  concentration in the nanocrystals causing an increase in the activation energy required for the hexagonal to orthorhombic phase transformation. Looking at the activation energies for the Eu-free ZBLAN, it is striking that the energies for both phases are within the error ( $E_{a,\text{hex.}} = 240 \pm 7$  kJ/mol and  $E_{a,\text{ortho.}} = 235 \pm 9$  kJ/mol), while there is a large difference between the hexagonal and the orthorhombic crystallization energy for the various Eu-doped samples (the maximum difference is 63 kJ/mol for an  $\text{Eu}^{2+}$  fraction of 0.39). This difference decreases with increasing  $\text{Eu}^{2+}$  fraction.

### 3.2. Rare-earth co-doping

$\text{Eu}^{2+}$ -doped glasses which are additionally doped with a further RE such as Gd, Nd, Yb, or Tb are interesting to investigate because of possible energy transfer processes between the two RE ions and potential effects on the luminescence properties. However, a further RE may also affect the  $\text{BaCl}_2$  crystallization which is investigated in detail below.

Figure 6 shows DSC data for the RE co-doped series and an undoped glass for comparison; the heating rate was 10 K/min. Besides the outlying crystallization peaks for the  $\text{Gd}^{3+}$ -doped glass (see below), the shift of the main crystallization peak of the undoped sample to lower temperatures is striking. This crystallization was attributed to a partial crystallization of the glass matrix, namely the formation of  $\beta\text{-BaZrF}_6$  and  $\text{NaZrF}_5$  [15]. It confirms the recently found behavior that higher fluorine content (lower fluorine evaporation during the melting process) leads to a decrease in peak temperature and an earlier crystallization, because more fluorine increases the probability for the crystals to form. Since the undoped sample was made as the only 20 g batch (the others were 10 g batches) less mass % of

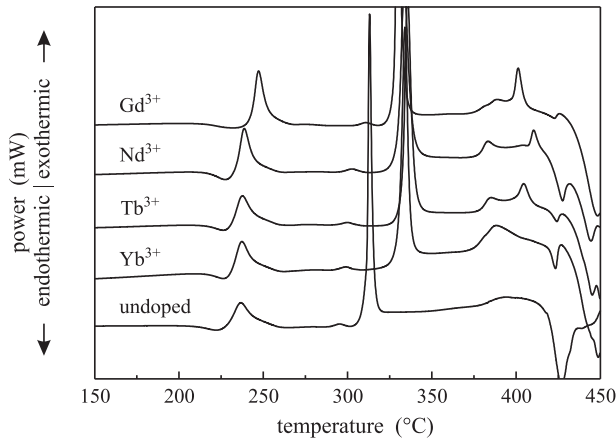


Figure 6: Plot of the DSC data for FCZ glasses with different RE co-dopants. The heating rate was 10 K/min. Data for an undoped ZBLAN glass is shown for comparison and the curves are vertically displaced for clarity.

fluorine was lost during the same melting process. This was established by ion chromatography measurements. The averaged crystallization temperature is 334 °C for the RE co-doped samples, while it is 313 °C for the undoped sample, i.e., the crystallization temperature is reduced by 21 °C. To give a clearer picture, the peak positions for hexagonal and orthorhombic phase crystallizations are also shown in Figure 7. As mentioned earlier for the multivalent Eu series, the temperature difference between both crystallization peaks slightly increases when the sample is doped with RE ions.

GdCl<sub>3</sub> as a co-dopant for EuCl<sub>2</sub> retards the nucleation and growth of BaCl<sub>2</sub> nanocrystals the most, as both crystal phases crystallize at the highest temperatures ( $T_{p1}(\text{Gd}^{3+}) = 247$  °C,  $T_{p2}(\text{Gd}^{3+}) = 311$  °C). Compared to the other co-dopants the cause of this is thought to be the larger atomic radius of Gd<sup>3+</sup> of about 233 pm ( $r_{\text{Tb}} = 225$  pm,  $r_{\text{Yb}} = 222$  pm and  $r_{\text{Nd}} = 206$  pm) [16] resulting in a higher electro-negativity and higher probability to attract electrons towards the nucleus. Therefore, more energy is needed to break the bond between the Gd and Cl ions or to split off chlorine ions, which can then contribute to the crystallization and growth of more and larger BaCl<sub>2</sub> nanocrystals. However, Nd<sup>3+</sup> does not fit into this trend, since its crystallization peak temperatures are in between the peaks of Gd<sup>3+</sup> and Tb<sup>3+</sup> and not, as one would suggest from the atomic radius, at the lowest temperature of all co-dopants. This effect can be explained by former studies on Nd<sup>3+</sup>-doped FCZ glasses and glass ceramics which have shown that the optical transitions of the Nd ions are affected by the BaCl<sub>2</sub> nanocrystal size leading to the conclusion that some of the Nd<sup>3+</sup> ions, similar to Eu<sup>2+</sup>, are sitting in close proximity to the nanocrystals or possibly incorporated into them [4]. Thus, the interactions between Nd ions and the BaCl<sub>2</sub> crystal lattice may lead to the higher BaCl<sub>2</sub> crystallization temperature.

Looking at the crystallization activation energies in Figure 8, Gd<sup>3+</sup> is once again outlying: Both hexagonal and orthorhombic crystallizations show a much lower activation energy than the undoped sample, especially for the orthorhombic crystallization

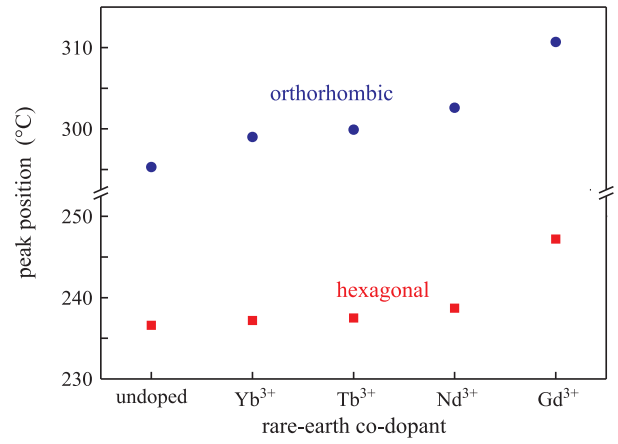


Figure 7: Crystallization peak position for the hexagonal (squares) and the orthorhombic BaCl<sub>2</sub> crystallization (circles) depending on the different RE dopants. The heating rate was 10 K/min. Data for an undoped ZBLAN glass is shown for comparison.

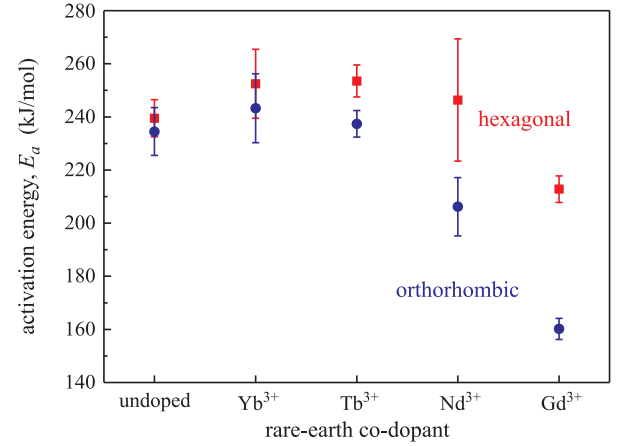


Figure 8: Hexagonal (squares) and orthorhombic (circles) BaCl<sub>2</sub> crystallization activation energies,  $E_a$ , obtained by Kissinger's method [12] for different RE co-dopants. Data for an undoped ZBLAN glass is shown for comparison.

with 160 kJ/mol compared to 235 kJ/mol for the undoped sample. Also, the difference in the activation energy of the hexagonal and orthorhombic crystallization is considerably larger: For Gd<sup>3+</sup> it is 53 kJ/mol, while it is only 5 kJ/mol for the undoped sample. The difference decreases for the row Nd<sup>3+</sup> (40 kJ/mol) via Tb<sup>3+</sup> (17 kJ/mol) to Yb<sup>3+</sup> (10 kJ/mol).

#### 4. Conclusion

DSC measurements have shown that the crystallization of hexagonal phase BaCl<sub>2</sub> is not very sensitive to different Eu oxidation states, while the hexagonal to orthorhombic phase transition shows increased activation energy,  $E_a$ , with increasing Eu<sup>2+</sup> doping fraction.

In order to increase total luminescence yield, Eu<sup>2+</sup>-doped FCZ glasses were additionally doped with Gd, Nd, Yb, or Tb chlorides. Influence on the nanocrystallization such as retar-

dation of nucleation and growth was observed. These crystallization shifts, in terms of temperature, could be attributed to the different atomic radii of the co-dopants associated with differences in electro-negativity.  $Gd^{3+}$  retarded nucleation and growth of  $BaCl_2$  nanocrystals the most as it has the largest atomic radius.  $Nd^{3+}$  did not fit into this trend, possibly due to stronger structural interactions between Nd ions and the  $BaCl_2$  crystal lattice, e.g. a possible incorporation into the nanocrystals; this was observed in previous work.

Future work will focus on the optical characterization of the RE co-doped glass ceramics as well as on a two-step annealing process, where in a first step as many nucleation grains as possible will be created, followed by an accurately defined growth to the desired crystallite size.

## Acknowledgment

C. Paßlick and S. Schweizer would like to thank the German Federal Ministry for Education and Research (BMBF) for financial support within the Centre for Innovation Competence SiLi-nano<sup>®</sup> (Project No. 03Z2HN11). In addition, S. Schweizer was supported by the FhG Internal Programs under Grant No. Attract 692 034.

The sample synthesis was supported by the National Institute of Biomedical Imaging and Bioengineering (NIBIB) under Grant No. 5R01EB006145-02 and the characterization was supported under National Science Foundation Award # DMR 1001381. The content is solely the responsibility of the authors and does not necessarily represent the official views of the National Science Foundation or the National Institutes of Health.

## References

- [1] J. A. Johnson, S. Schweizer, B. Henke, G. Chen, J. Woodford, P. J. Newman, D. R. MacFarlane, Eu-activated fluorochlorozirconate glass-ceramic scintillators, *J. Appl. Phys.* 100 (2006) 034701.
- [2] J. A. Johnson, S. Schweizer, A. R. Lubinsky, A Glass-Ceramic Plate for Mammography, *J. Am. Ceram. Soc.* 90 (3) (2007) 693–698.
- [3] B. Ahrens, B. Henke, P. T. Miclea, J. A. Johnson, S. Schweizer, Enhanced up-converted fluorescence in fluorozirconate based glass ceramics for high efficiency solar cells, *Proc. of SPIE: Photonics for Solar Energy Systems II* 7002 (2008) 700206.
- [4] B. Ahrens, P. Löper, J. C. Goldschmidt, S. Glunz, B. Henke, P. T. Miclea, S. Schweizer, Neodymium-doped fluorochlorozirconate glasses as an up-conversion model system for high efficiency solar cells, *physica status solidi (a)* 205 (12) (2008) 2822–2830.
- [5] C. Paßlick, B. Henke, B. Ahrens, P. T. Miclea, J. Wenzel, E. Reisacher, W. Pfeiffer, J. A. Johnson, S. Schweizer, Glass-ceramic covers for highly efficient solar cells, *SPIE Newsroom*.
- [6] C. Paßlick, B. Ahrens, B. Henke, J. A. Johnson, S. Schweizer, Crystallization behavior of rare-earth doped fluorochlorozirconate glasses, *J. Non-Cryst. Solids* 357 (11-13) (2011) 2450–2452.
- [7] D. R. MacFarlane, M. Matecki, M. Poulain, Crystallization in fluoride glasses: I. Devitrification on reheating, *Journal of Non-Crystalline Solids* 64 (3) (1984) 351–362.
- [8] M. Poulain, Overview of crystallization in fluoride glasses, *Journal of Non-Crystalline Solids* 140 (1992) 1–9.
- [9] J. K. R. Weber, M. Vu, C. Paßlick, S. Schweizer, D. E. Brown, J. C. E., J. J. A., The oxidation state of europium in halide glasses, *J. Phys.: Condens. Matter* 23 (2011) 495402.
- [10] C. Paßlick, O. Müller, D. Lützenkirchen-Hecht, R. Frahm, J. A. Johnson, S. Schweizer, Structural properties of fluorozirconate-based glass ceramics doped with multivalent europium, *J. Appl. Phys.* 110 (2011) 113527.
- [11] I. D. Aggarwal, G. Lu (Eds.), *Fluoride Glass Fibre Optics*, Academic Press, London, 1991.
- [12] H. E. Kissinger, Reaction Kinetics in Differential Thermal Analysis, *Anal. Chem.* 29 (11) (1957) 1702–1706.
- [13] S. Schweizer, L. W. Hobbs, M. Secu, J.-M. Spaeth, A. Edgar, G. V. M. Williams, J. Hamlin, Photostimulated luminescence from fluorochlorozirconate glass ceramics and the effect of crystallite size, *J. Appl. Phys.* 97 (2005) 083522.
- [14] H. Wever, H. W. Den Hartog, EPR of  $BaCl_2:Eu^{2+}$  and  $BaCl_2:Gd^{3+}$ , *physica status solidi (b)* 70 (1) (1975) 253262.
- [15] M. Baricco, L. Battezzati, M. Braglia, G. Cocito, J. Kraus, E. Modone, Crystallization behaviour of fluorozirconate glasses, *J. Non-Cryst. Solids* 161 (1993) 60–65.
- [16] E. Clementi, D. L. Raimondi, W. P. Reinhardt, Atomic Screening Constants from SCF Functions. II. Atoms with 37 to 86 Electrons, *J. Chem. Phys.* 47 (1967) 1300–1307.